ORIGINAL ARTICLE

Preparation of gamma cyclodextrin stabilized solid lipid nanoparticles (SLNS) using stearic acid–γ-cyclodextrin inclusion complex

Jeetendra Singh Negi · Pronobesh Chattopadhyay · Ashok Kumar Sharma · Veerma Ram

Abstract The inclusion complexation behaviour of higher chain fatty acid, stearic acid (SA) with gamma cyclodextrin has been investigated. The inclusion complex was characterized by FT-IR, ^{1}H NMR, 2D NMR, XRD and DSC techniques. The results showed that the SA molecule was entrapped inside the gamma cyclodextrin cavity. Further, inclusion complex was treated with lopinavir at 85 °C and emulsified with hot water at 85 °C. The resulted nanoemulsion was cooled down to form solid lipid nanoparticles (SLNs) stabilized with gamma cyclodextrin. Prepared SLNs were having average particle size of 212.5 ± 4.8 nm, zeta potential of −19.7 ± 0.66 mV and drug loading of 57.54 ± 0.62 %. The surface characteristics of SLNs were also observed with transmission electron microscopy and atomic force microscopy. Results indicate that inclusion complex of SA and gamma cyclodextrin can be used for SLNs preparation.

J. S. Negi (✉) · V. Ram
Department of Pharmaceutical Sciences, S Bhagwan Singh PG Institute of Bio-medical Sciences and Research, Balawala, Dehradun 248161, Uttarakhand, India
e-mail: rx.jnegi@gmail.com

P. Chattopadhyay
Division of Pharmaceutical Technology, Defence Research Laboratory, Tezpur 784 001, Assam, India

A. K. Sharma
Institute of Pharmacy, Ministry of Health, Asmara, Government of Eritrea

Introduction

Cyclodextrins are macrocyclic oligosaccharide molecules having repeated α-D-glucopyranoside units to form truncated cone shape structure. The exterior region of cone is hydrophilic due to the outer orientation of hydroxyl groups. In contrast, the interior cavity of cyclodextrins remains hydrophobic due to the inner orientation of hydrocarbon moiety of glucopyranoside units. The hydrophobic cavity of cyclodextrin molecule can encapsulate various lipophilic molecules by forming inclusion complex with them [1, 2]. This improves aqueous solubility and chemical stability of guest molecules. Recently Sun et al. [3] prepared supramolecular amphiphiles having hydrophilic head of cyclodextrins and hydrophobic tail of guest molecule. These supramolecular amphiphiles were assembled to form vesicular drug delivery system. Similarly Messner et al. [4] also reported aggregation or self-assembly tendency of inclusion complex of lipophilic drug molecules and cyclodextrin. Present study investigates formation of inclusion complex of stearic acid (SA) with γ-cyclodextrin (γ-CD) and its application in SLNs formation for drug delivery. SA has been widely used for preparation of solid lipid nanoparticles (SLNs) by several researchers in recent past [5, 6]. Generally, SA is nano-emulsified with hot water in presence of suitable surfactant. The surfactant stabilized nanoemulsion is then cooled down for formation of SLNs. γ-CD was selected due to its largest cavity as well as higher aqueous solubility in comparison to other natural cyclodextrins. The inclusion complex of SA with γ-CD was

nanoemulsified in hot water without presence of surfactant. The nanoemulsion stabilized with γ-CD was further cooled down to form γ-CD stabilized SLNs. This approach also excludes the requirement of surfactant for SLNs formation. The SLNs were characterized by particle size, zeta potential, transmission electron microscopy (TEM) and atomic force microscopy (AFM) analysis. Lopinavir (LOP) was selected as model drug for SLNs formulation. In recent past, SLNs formulations of LOP has been developed for improvement of its low oral bioavailability [7, 8]. SLNs formulation of LOP can bypass P-glycoprotein efflux transport and first pass metabolism by CYP450 3A enzyme. It also provides ritonavir free strategy for bioavailability enhancement of LOP [9].

Materials and methods

Materials

LOP was obtained as generous gift sample from Matrix laboratories Ltd., Hyderabad (India). SA was purchased from Sigma-Aldrich (India). Gamma cyclodextrin was obtained from Jubilent Life Sciences, Noida (India). Dialysis bag of 12–16 kD were purchase from Himedia ltd (India). Other chemicals and solvents used were of analytical grades.

Preparation of stearic acid–γ-cyclodextrin inclusion complex

Inclusion complex of SA with γ-CD was prepared by a solution-ultrasonic method [10, 11]. SA and γ-CD (1:1 molar ratio) were completely dissolved in a 95 % v/v mixture of absolute ethanol and water. The solution was kept in ultrasonic bath for next 3 h at room temperature in the dark. Finally solution was filtered through 0.45 micron membrane filter and filtrate was evaporated under reduced pressure and dried in a vaccum oven to obtain SA–γ-CD inclusion complex.

Characterization of SA–γ-CD inclusion complex

The complex was characterized by FTIR, NMR and XRD. FT-IR spectra were obtained by pressing samples into KBr pellets and recorded at frequencies from 4,000 to 200 cm^{-1} using Perkin-Elmer Paragon 1000 spectrometer. For XRD studies, samples were scanned from 5° 2θ to 50° 2θ with Cu Kα radiation generated at 40 mA, 35 kV in X'Pert Powder PANalytical X-ray diffractometer. ^{1}H NMR spectra of SA, γ-CD and SA–γ-CD inclusion complex were recorded in D$_2$O solvent using Bruker 500 MHz spectrometer. DSC was carried out using EXSTAR TG/DTA

6300. A mass of 10 mg samples were accurately weighted, sealed in an aluminium pan with nitrogen environment [Nitrogen (200 ml/min)] and equilibrated at 25 °C, which were subjected to a heating run over the temperature range of 25–350 °C.

Molecular docking study

The molecular docking study was performed for finding best probable structure of SA–γ-CD inclusion complex using Autodock Vina [12]. The 3D structure of SA and CD were obtained by using SMILES formulas generated by CORINA server [13]. The ligand and receptor files were processed using the Autodock Tools.

Preparation of SLNs using SA–γ-CD inclusion complex

The SLNs were prepared by hot homogenization method. Accurately weighed quantity of LOP was added to the SA–γ-CD inclusion complex previously kept at 85 °C and mixed well with help of glass rod. The hot aqueous solution was added to the complex drug mixture and homogenized at 10,000 rpm for 10 min using high speed homogenizer [14]. The temperature of the system was kept constant at 85 °C during homogenization. Resulted nanoemulsion was then instantly cooled in an ice bath for solidification of nanodroplets of SA into SLNs. The SLNs dispersion was centrifuged at 14,000 rpm for 30 min using cooling centrifuge. Purified SLNs were redispersed in 50 ml distilled water and freeze dried at vaccum pressure 0.77 mBar and −84 °C temperature using Labconco Freeze 4.5 freeze dryer. Freeze dried SLNs were further stored at 4 °C.

Particle size analysis and zeta potential measurements

The average particle size and polydispersity index (PDI) of SLNs were determined by differential light scattering (DLS) technique using Malvern Zetasizer (Nano ZS90, Malvern instrument Ltd., UK). One ml SLNs dispersion was diluted up to 10 ml with distilled water to reduce opalescence during particle size measurement [15]. Malvern Zetasizer (Nano ZS90, Malvern instrument Ltd., UK) was also used for zeta potential measurement of SLNs based on the Smoluchowski equation and operated at 25 °C with electrical field strength of 23 V/cm.

Entrapment efficiency and drug loading of SLNs

The encapsulation efficiency (EE) of SLNs was calculated by determining the remaining un-entrapped amount of LOP of the aqueous surfactant solution after Lopinavir loaded SLN (LOP-SLNs) formation [16]. LOP-SLNs were then centrifuged at 14,000 rpm for 30 min in a cooling centrifuge

and the filtrate was diluted and analyzed by HPLC [17]. EE was determined using the following formula:

$$EE = \frac{Amount\ of\ LOP\ in\ SLNs}{Total\ weight\ of\ LOP} \times 100 \qquad (1)$$

Drug loading was determined by estimating concentration of LOP in 100 mg freeze dried SLNs using following formula.

$$Drug\ loading = \frac{Amount\ of\ LOP\ in\ SLNs}{Weight\ of\ Lipid\ in\ SLNs} \times 100 \qquad (2)$$

Transmission electron microscopy (TEM) of SLNs

TEM (H-7500, Hitachi, Japan) was employed to study the morphology of the resulting SLNs. Staining of SLNs with 1 % (w/v) phosphotungstic acid was done before observation.

Atomic force microscopy (AFM) of SLNs

AFM images of LOP-SLNs were recorded with a confocal laser dispersion Raman microscope integrated with AFM Microscope (Multiview 1000™, Nanonics Imaging Ltd, Israel). Freeze-dried SLNs were dispersed in double distilled water and after appropriate dilution spread as a thin film on a mica sheet [18]. The samples were then allowed to air dry for 24 h and AFM images were recorded.

In-vitro release studies

SLNs dispersion equivalent to 50 mg LOP was kept inside a dialysis tubing with both ends were tightly sealed. This sealed dialysis tube was place in a 250 ml beaker containing 0.1 N HCl (pH 1.2) and magnetically stirred at 100 rpm for next 2 h. After 2 h dialysis tube was withdrawn and placed into another beaker containing 100 ml Phosphate buffer pH 6.8 for next 12 h [19]. Samples were withdrawn at different time interval and after filtration mixed with methanol and mobile phase (80:20 v/v) for analysis using HPLC at 210 nm.

Results and discussion

The γ-CD-SA-inclusion complex was prepared by solution-sonication method. For inclusion complex formation both SA and CD must interact at molecular level. Due to
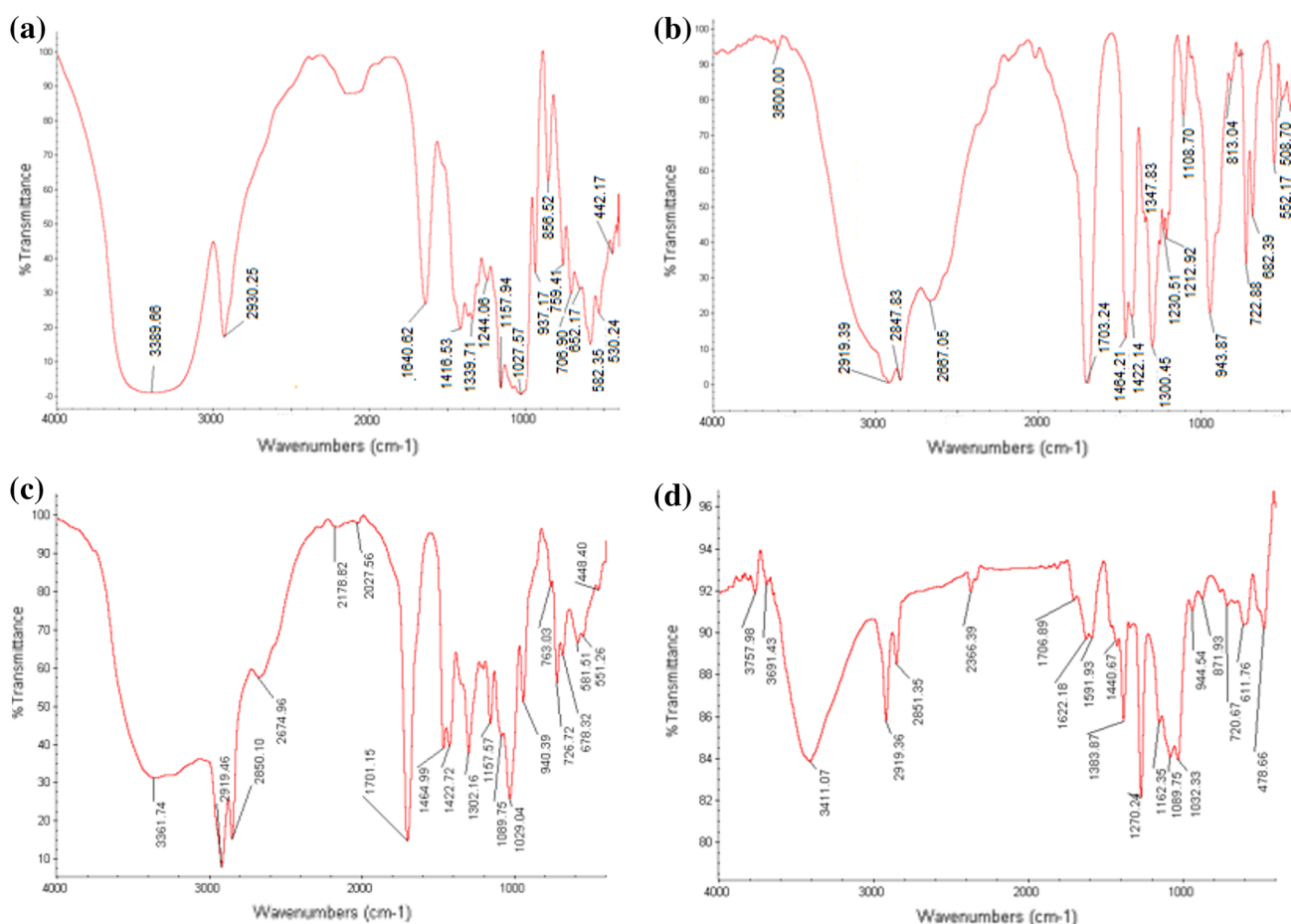

Fig. 1 FT-IR spectra of a γ-CD, b SA, c physical mixture (1:1) of γ-CD & SA and d SA–γ-CD inclusion complex

insolubility of SA in water, 95 % ethanol solution was selected as solvent system. The molecular interaction between γ-CD and SA was further facilitated by sonication for next 3 h. After sonication the mixture was evaporated and dried in vaccum oven to obtain solid inclusion complex.

The complexation between γ-CD and SA was further characterized by FT-IR study. The FT-IR spectra of pure γ-CD, pure SA, physical mixture and SA–γ-CD inclusion complex are shown in Fig. 1. Some important assigned peaks are given in Table 1. Pure SA spectrum was characterized by presence of peaks for terminal carboxyl group at 1,703.24 cm^{-1} for carbonyl stretching, at 1,300.45 cm^{-1} for C–O stretching and at 1,422 cm^{-1} for C–O–H in plane bending. Other SA peaks for methylene groups were also present at 2,919 cm^{-1} for asymmetric stretching, at 2,847 cm^{-1} for symmetric stretching and at 1,464.21, 722 cm^{-1} for in plane bending. The FI-IR spectrum of physical mixture was superimposition of pure SA and γ-CD spectra. However in inclusion complex spectrum, the intensity of SA peaks was reduced significantly. The reduction in intensity was might be due to masking of SA groups due to formation of inclusion complex. The absorption bands at 1,464.21 cm^{-1} for methylene groups of SA was shifted to low wavenumber, 1,440.67 cm^{-1} in inclusion complex that indicates possibility of methylene chain association with hydrophobic cavity of γ-CD [20]. In FT-IR spectrum of inclusion complex the carbonyl stretching of SA carboxylic group was shifted to 1,706.89 cm^{-1} with significant reduction in intensity. This indicates carbonyl stretching of carboxyl group of SA was restricted due to inclusion inside γ-CD cavity [21]. Moreover, C–O stretching at 1,300 cm^{-1} was not observed in FT-IR spectrum of complex which further confirms change in environment of carboxyl group due to inclusion complex formation. Thus FT-IR results indicate carboxylic end of SA might entrapped inside the γ-CD cavity.

XRD patterns of γ-CD, SA, physical mixture and SA–γ-CD inclusion complex are shown in Fig. 2. Diffraction pattern of pure SA was characterized by sharp intense peaks at 21.94 and 24.57 2θ. These peaks denote β/β' polymorphic forms with orthorhombic structure of SA [22]. Similarly distinctive peaks at 11.6, 13.8, 14.95 16.34 and 21.7 2θ were present in pure γ-CD diffraction pattern. In physical mixture all the characteristic peaks of SA and γ-CD were present with their respective intensity. The 2θ value of characteristic peaks of SA and γ-CD were shifted in inclusion complex pattern which indicates change in environment due to inclusion complex formation. The SA peaks intensity was also reduced significantly in XRD pattern of complex which might suggest the reduction in crystallinity of SA. However, no significant reduction in γ-CD peaks intensity was observed which suggested γ-CD remained crystalline after complexation.

The inclusion complex formation can be assessed by chemical shift displacement and line broadening of ^{1}H NMR spectral signals of host and guest protons [23]. The values of chemical shifts for different protons of SA, γ-CD and inclusion complex are given in Table 2. Figure 3 shows ^{1}H NMR spectra of SA, γ-CD and SA–γ-CD inclusion complex in DMSO-d$_6$. The ^{1}H NMR spectrum of SA contained characteristic peaks at δ 2.17 ppm for C2 methylene, at δ 1.47 ppm for C3 methylene and at δ 0.85 ppm for terminal methyl protons. The characteristic intense peak at δ 1.23 ppm was assigned to 28 protons of C4–C17 methylene groups of SA [24]. Similarly the ^{1}H NMR spectrum of the γ-CD was characterized by triplet at δ 4.5 ppm for C6–OH proton, doublet at δ 5.7 ppm for C2–OH and C3–OH protons, respectively. Other peaks for γ-CD protons were also similar to that reported by Gonil et al. [25]. The displacement in chemical shifts was observed for SA and γ-CD protons in ^{1}H NMR spectrum of inclusion complex. As shown in Table 2, a minimal displacement in chemical shift values was observed for outside protons of γ-CD (H-1, H-2 and H-4). Inclusion of SA molecule must be associated with chemical shift changes of the inside protons (H3 & H5) of γ-CD [21]. The major displacement in chemical shift was observed for H3 and H5 protons of γ-CD. This indicates, the inclusion of SA molecule was resulted in de-shielding of H3 and H-5 proton with down field shift. Further, change in chemical shift was

Table 1 Wavenumbers (cm^{-1}) from FTIR spectra of SA and γ-CD

| SA	γ-CD
3,300–2,500 broad O–H stretching	3,389.66 cm^{-1}: asymmetric and symmetric stretching (v_{as}, v_s) of OH
2,919.39 cm^{-1}: assymetric stretching (v_{as}, C–H) from CH$_2$	2,930.25 cm^{-1}: asymmetric stretching (v_{as}, C–H) from CH$_2$
2,847.83 cm^{-1}: symmetric stretching (v_s, C–H) from CH$_2$	1,416.53 cm^{-1}: in plane bending, scissoring (δ_{as}, C–H) from CH$_2$
1,703.24 cm^{-1}: C=O stretching of carboxylic group	1,339.71 cm^{-1}: coupled in plane bending δ_s (C–H) of CH$_2$; δ O–H
1,464.21 cm^{-1}: in plane bending, δ_s (C–H) of CH$_2$	1,089.56, 1,157.94 cm^{-1}: in plane bending δ_{as} C-0-C
1,422.14 cm^{-1}: in plane bending, δ_s O–H	1,027.57 cm^{-1}: stretching for (C–C–O) C–OH
1,300.45 cm^{-1}: C–O stretching of C–OH	937.17 cm^{-1}: skeletal vibration involving α-1,4 linkage
943.87 cm^{-1}: O–H out of plane bending	856.52 cm^{-1}: δ (C–C–H), (C–O), (C–C) from anomeric vibration
722.88 cm^{-1}: in plane bending, rocking (ρ C–H) of CH$_2$	
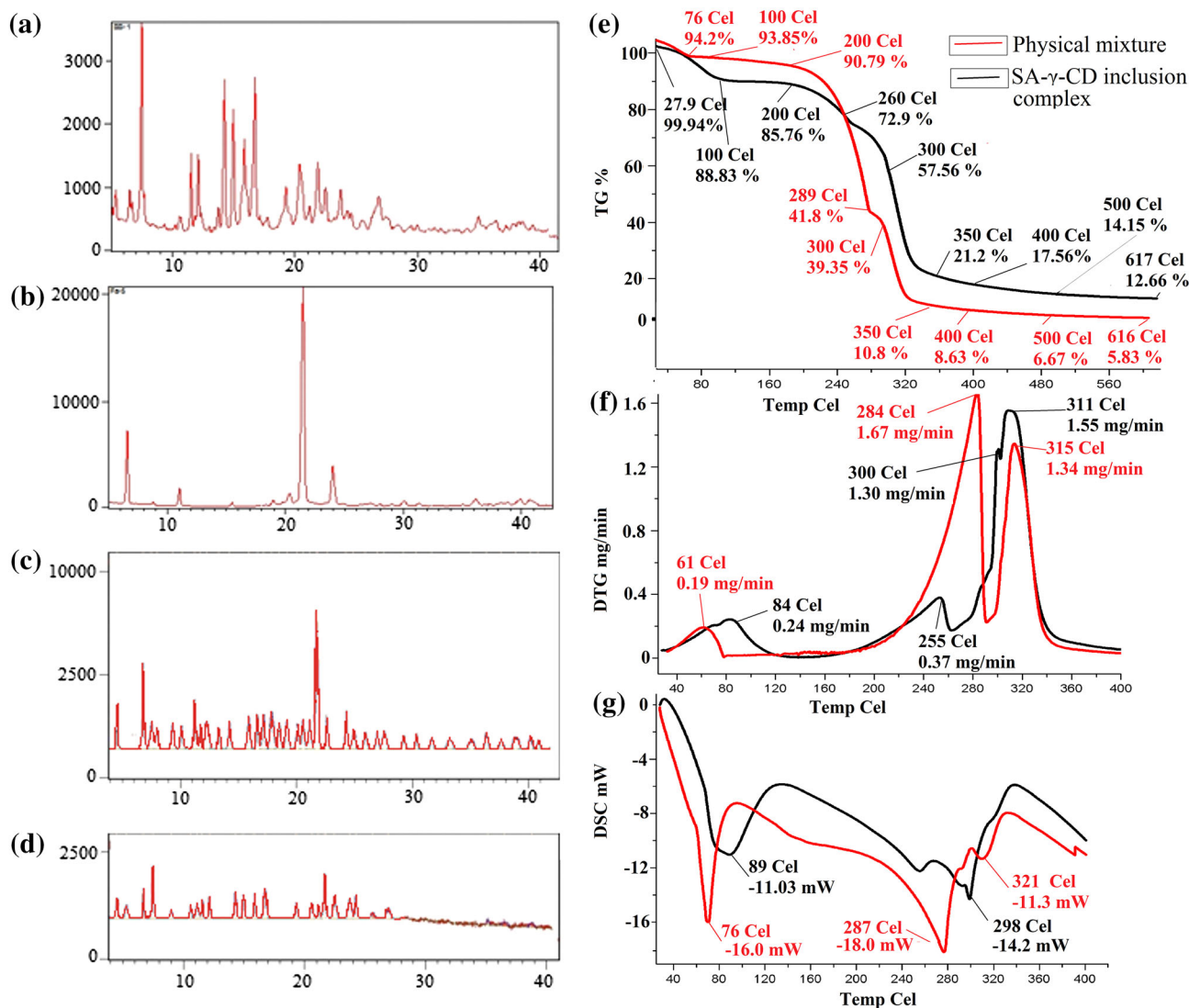
Fig. 2 XRD patterns of **a** γ-CD, **b** SA, **c** physical mixture (1:1) of γ-CD & SA and **d** SA–γ-CD inclusion complex and thermal profile of **e** TG curve **f** DTG curve **g** DSC curve of physical mixture (1:1) of γ-CD & SA and SA–γ-CD inclusion complex

observed for all methylene and methyl protons of SA. This indicates long chain fatty acid, SA, was included in γ-CD cavity.

To obtain further information of inclusion complex formation, 2D ROESY spectrum were recorded. 2D spectrum gives idea about interaction between host and guest molecules in the complex and the connectivity between neighbour protons. The ROESY spectra further extend the understanding given by 1D NMR by providing information regarding the spatial proximity of host and guest atoms. In 2D ROESY, two closely located protons in space create a nuclear over hauser effect (NOE). The NOE cross peaks presence for different protons indicates spatial contacts within 3–4 Å [11]. The ROESY spectrum of complex showed appreciable correlation of C4–C16 protons with H3

and H5 protons of γ-CD (red inset Fig. 4). However, assignment of interaction peaks inside the cavity of γ-CD is difficult due to overlapping of H3, H5 and H6 protons of γ-CD [26]. Further, a weak NOE correlation peak was also observed for C2 proton of SA with H5 proton of γ-CD (green inset Fig. 4). This weak cross peak suggested that carboxylic end was also included inside the narrow end of γ-CD cavity.

Thermal behaviour of physical mixture in molar ratio 1:1 and inclusion complex are shown in Fig. 2e. Thermogravimetric curve of physical mixture was characterized with initial 6 % loss of water molecules [27] from γ-CD (50–100 °C) followed by two step decomposition events. First decomposition with 50 % loss from 200 to 289 °C was due to decomposition of SA [28] and second

Table 2 Chemical shifts (ppm) and chemical shift variation ($\Delta\delta$) from ^{1}H NMR spectra of SA and γ-CD with reference to SA–γ-CD inclusion complex (a, b, c & d indicates corresponding protons of SA as shown in Fig. 3b)

γ-CD		SA–γ-CD inclusion complex	$\Delta\delta$	SA		SA–γ-CD inclusion complex	$\Delta\delta$
C2–OH	5.7766	5.7778	0.0012	d	0.8528	0.8661	0.0133
C3–OH	5.7526	5.7533	0.0007	c	1.2335	1.2467	0.0132
H1	4.8904	4.8912	0.0008	b	1.4744	1.4939	0.0195
C6–OH	4.5527	4.5536	0.0009	a	2.1783	2.191	0.0127
H6	3.6231	3.625	0.0019				
H3	3.5979	3.613	0.0151				
H5	3.5199	3.5349	0.015				
H4	3.3508	3.3518	0.001				
H2	3.3274	3.3281	0.0007				

decomposition with 30 % from 300 to 350 °C was due to decomposition of γ-CD [29]. In thermogravimetric curve of inclusion complex the decomposition of SA occurs from 200 to 260 °C with only 13 % loss. This might be due to inclusion of SA molecule inside the γ-CD cavity which prevented SA molecule decomposition. However the decomposition of γ-CD was not affected by much. Similar

results were observed in DTG curve of inclusion complex where decomposition rate of SA was found 0.37 mg/min in comparison to 1.66 mg/min for physical mixture (Fig. 2f). Further DSC curve of physical mixture was characterized by sharp endothermic peak at 76 °C for SA melting point and at 287 °C for melting point of γ-CD (Fig. 2g). The γ-CD melting peak was shifted to 298 °C after complexation which indicates change in environment of γ-CD due to inclusion complexation. Also, a broad endothermic peak for SA with reduction in intensity was observed in DSC curve of complex. This change in melting behaviour of SA suggested the inclusion of SA molecule inside the cyclodextrin cavity.

The Autodock Vina provided nine different orientations with their binding affinity. The orientation with minimum binding energy was considered best possibility by Autodock Vina. The docking views of γ-CD with SA are shown in Fig. 5. The docking view suggested that the carboxylic end of SA was present at narrow end of γ-CD cavity. The long methylene chain was coiled inside the cavity in such a manner that terminal methyl group was present at broad end of γ-CD cavity. These results were in conformity with IR results where restriction in carbonyl stretching of SA was observed in IR spectra of SA–γ-CD inclusion complex. Unlike several other docking programs, Autodock
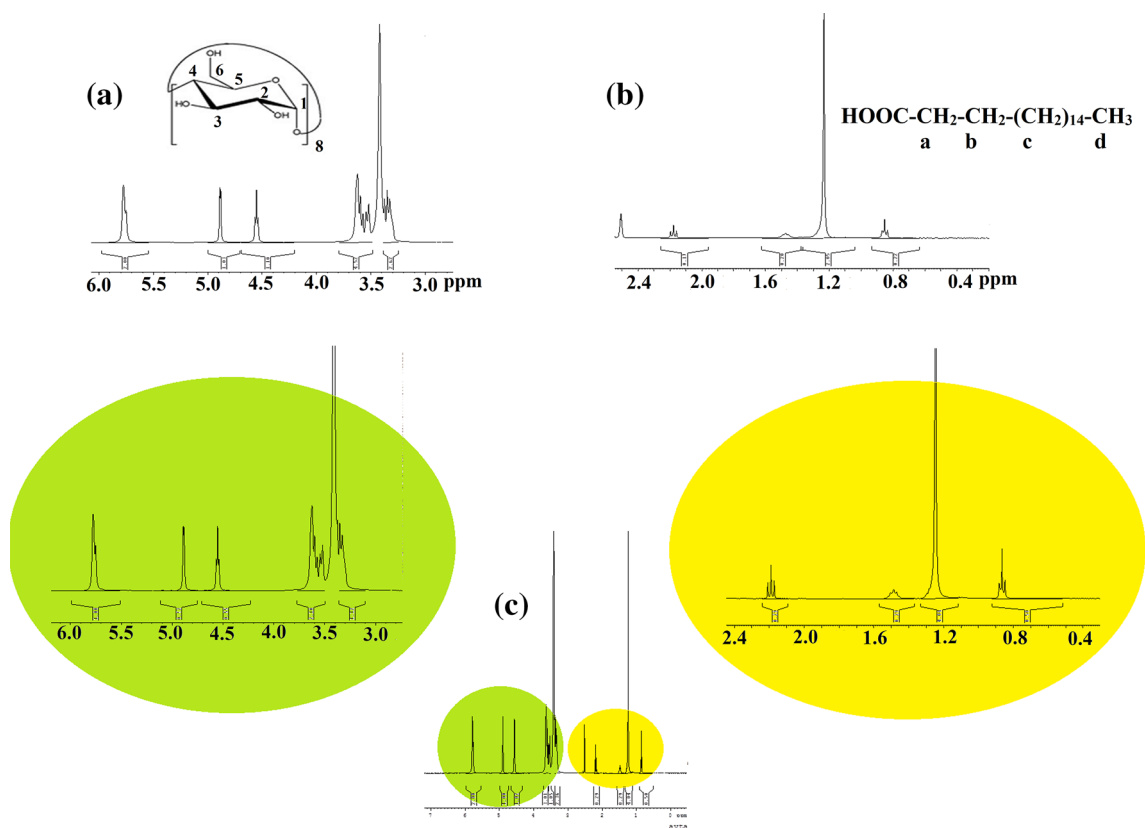

Fig. 3 ^{1}H NMR spectra of **a** γ-CD, **b** SA and **c** SA–γ-CD inclusion complex
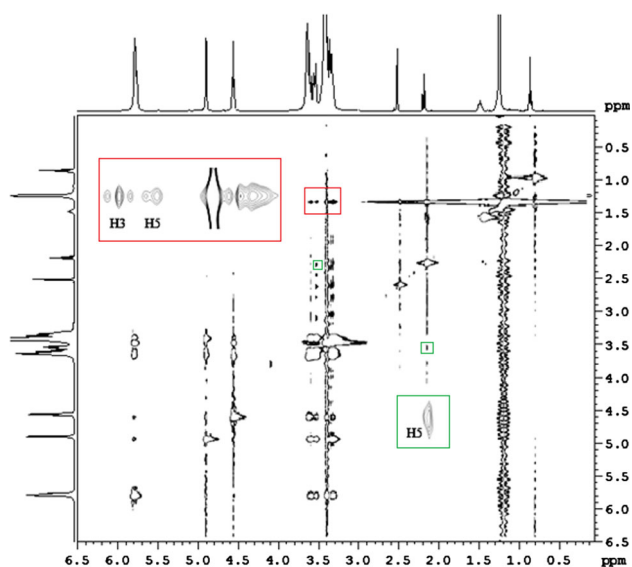
Fig. 4 2D ROSEY spectra of SA–γ-CD inclusion complex

in chemical shifts was observed for all protons of SA in ^{1}H NMR spectra of complex.

Generally SLNs were prepared by hot emulsification of lipid in aqueous phase followed by solidification due to cooling. The surfactant molecules were necessary for emulsification as well as stabilization of SLNs. In present study an amphiphilic system in the form of SA–γ-CD inclusion complex was used instead of pure SA and surfactants. As inclusion complex was homogenized in hot water, a blue-white dispersion was obtained and no separation was observed after subsequent cooling of hot dispersion. In contrast when pure SA was homogenized in hot water, separation of lipid phase as separate layer was observed. This behaviour suggested that amphiphilic system remain stable at 85 °C and also form stable SLNs. Such behaviour of SLNs formation from SA–γ-CD inclusion complex has not been reported earlier. The reason for SLNs formation might be the tendency of amphiphilic system to form lipid rich droplets surrounded by hydrophilic γ-CD portion in hot water. Sun et al. [3] also reported similar tendency of spherical vesicle formation with "supramolecular amphiphiles" prepared by inclusion complex of β-CD and antharquinone derivatives. Simultaneous high speed homogenization was kept these droplets in nanosize range and resulted in formation of oil in water (o/w) hot nanoemulsion. Similarly Klang et al. [30] were also found that addition of γ-CD promoted the formation of

Vina considered the rotational bonds during exhaustive calculation of docking possibilities. SA molecule contains rotational sigma bonds in long methylene chain. The Autodock Vina was suggested coiling of whole methylene chain inside γ-CD cavity due to presence of rotational sigma bonds in SA molecule. This entrapment of whole SA molecule also supported by ^{1}H NMR results where change

Fig. 5 Molecular docking view of SA–γ-CD inclusion complex **a** *side and top* view with γ-CD in wireframes **b** *side and top* view with γ-CD in molecular surface mode
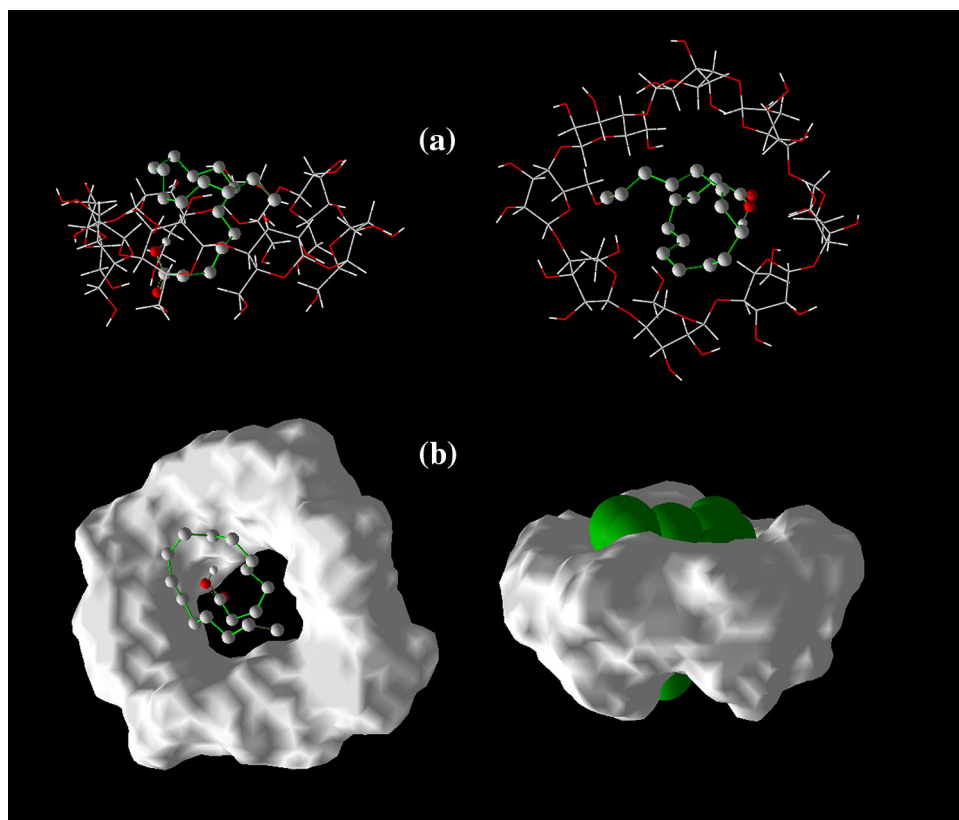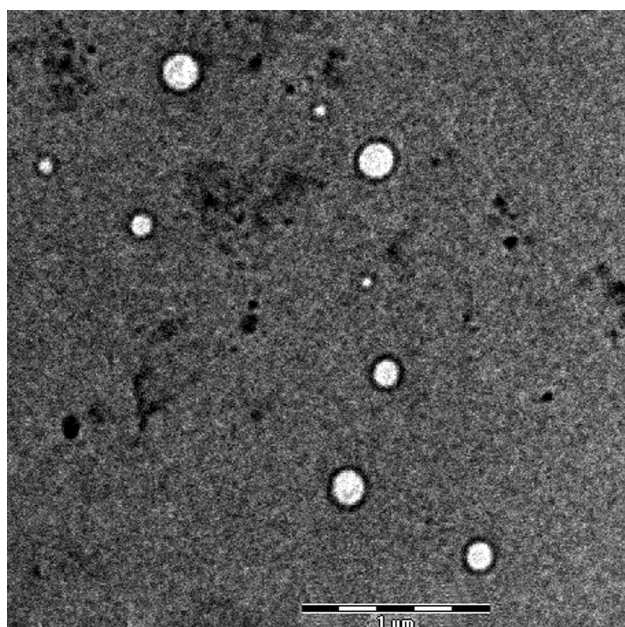
Fig. 6 TEM image of SLNs prepared using SA–γ-CD inclusion complex

nanoemulsion droplets. Further temperature reduction was resulted in SLNs formation due to solidification of SA nanodroplets. The resulted SLNs must be stabilized by γ-CD portion at periphery. For preparation of LOP loaded SLNs, the LOP was first treated with inclusion complex at 85 °C for allowing drug interaction with molten SA portion of inclusion complex. LOP must have higher affinity for molten SA portion of inclusion complex than CD portion due to higher lipophilic nature of SA than CD cavity. Further, LOP treated inclusion complex was emulsified in hot water by homogenization with subsequent cooling to form LOP loaded SLNs. The lipid portion entrapped the drug and formed SLNs whereas γ-CD portion of inclusion complex was presented at periphery to stabilize the SLNs. The average particle size of 199.8 ± 3.7 nm for unloaded SLNs and 212.5 ± 4.8 nm for LOP loaded SLNs were obtained from DLS study. Size range below 300 nm is considered suitable for absorption across Peyer's patches and villi of the gastrointestinal tract [31, 32]. High negative or positive value of zeta potential is considered as good indication of SLNs stability due to repulsion of same charge species. The zeta potential of drug loaded SLNs was
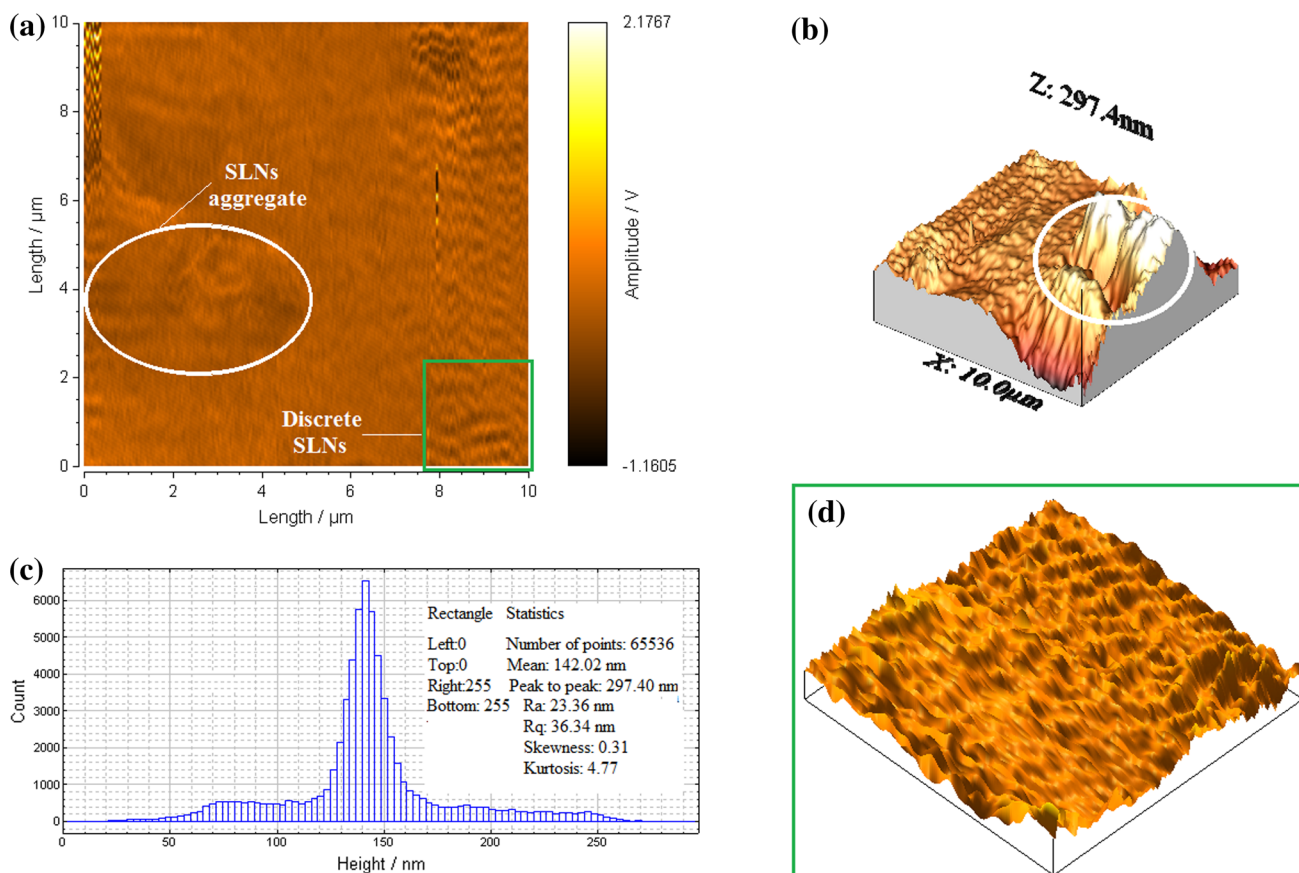

Fig. 7 AFM images of SLNs prepared using SA–γ-CD inclusion complex **a** planner amplitude image, **b** 3D height image, **c** Height distribution, **d** 3D view of *green inset*. (Color figure online)

found -19.7 ± 0.66 mV and indicates the good stability characteristics [33]. The entrapment efficiency of 95.91 ± 1.04 % and drug loading of 57.54 ± 0.62 % were observed for LOP loaded SLNs. In our previous study [9], with surfactant stabilized SLNs of SA, similar results were observed for particle size (180.6 ± 2.32 nm) zeta potential (-13.4 ± 0.56 mV) and drug loading (50 % $\pm$ 0.58). Further surface morphology of SLNs were investigated using TEM analysis. As shown in Fig. 6, white spherical particles were observed in dark background due to negative staining. The shape of SLNs was found more spherical than observed with surfactant stabilized SLNs reported previously. This might be due to the uniform packing of γ-CD rings around particles to stabilize them. Figure 7 shows AFM planner and 3D images of SLNs. AFM can provide information on morphology and size distribution of nanoparticles [34]. The washing of deposited SLNs sample with distilled water was done to remove larger aggregates of SLNs from mica sheet. Due to washing, only few small aggregates of SLNs (white circle in Fig. 7a) were observed in left corner. As shown in Fig. 7a, discrete layer of SLNs was present (green inset) with spherical shape. Further inspection of 3D images (Fig. 7b, d) indicates uniform distribution of nanoparticles with smooth surface. The maximum height of 297.4 nm was observed due to SLNs aggregates (white circle in Fig. 7b) as shown in 3D image. The mean particle height (Fig. 7c) for whole scan was 140.2 nm which is smaller than DLS results. This height decrease might be due to flattening of SLNs on mica sheet after deposition.

Further in vitro drug release studies were performed for LOP-SLNs. The dispersion was packed inside the dialysis bag and placed in acidic medium for first 2 h and basic medium for remaining time period under continuous stirring. Drug release in 0.1 N HCl after 2 h was 8 ± 1.1 % and in phosphate buffer after 12 h was 17 ± 2.5 %. Similarly, <15 % of drug release was observed in earlier work from surfactant stabilized SLNs of SA [9]. Drug release of small fraction after 12 h from SLNs indicates homogeneous dispersion of drug in lipid matrix and most fraction of the drug remain available in SLNs for GI uptake. After 4 month storage of freeze dried SLNs, no significant change in particle size (<20 nm) and drug release (<4 %) was observed. This indicates good stability of freeze dried SLNs at 4 °C. Similar stability profile for surfactant reduced SLNs was reported earlier [8].

Conclusions

Previous reports have demonstrated the formation of inclusion complex between cyclodextrin and drug molecules for improvement of drugs aqueous solubility. However few studies have been reported amphiphilic behaviour of cyclodextrins complex. Present study reported the formation of inclusion complex between long chain fatty acid, SA with γ-CD. The SLNs were prepared by hot emulsification technique using SA–γ-CD inclusion complex. A lipophilic drug LOP was also successfully entrapped inside the SLNs. The SLNs formation was confirmed by DLS, TEM and AFM analysis. The prepared SLNs must be stabilized by γ-CD at the periphery. Thus a surfactant free strategy for SLNs preparation was successfully developed using SA–γ-CD inclusion complex for delivery of lipophilic drugs.

References

1. Loftsson, T., Duchene, D.: Cyclodextrins and their pharmaceutical applications. Int. J. Pharm. **329**, 1–11 (2007)
2. Rowe, R.C., Sheskey, P.J., Weller, P.J., Quinn, M.E.: Handbook of Pharmaceutical Excipients, 6th edn. The Pharmaceutical Press, London (2009)
3. Sun, T., Li, Y., Zhang, H., Li, J., Xin, F., Kong, L., Hao, A.: pH-reversible vesicles based on the "supramolecular amphiphilies" formed by cyclodextrin and anthraquinone derivate. Colloid Surf. A **375**, 87–96 (2011)
4. Messner, M., Kukov, S.V., Brewster, M.E., Jansook, P., Loftsson, T.: Self-assembly of cyclodextrin complexes: aggregation of hydrocortisone/cyclodextrin complexes. Int. J. Pharm. **407**, 174–183 (2011)
5. Paliwal, R., Rai, S., Vaidya, B., Khatri, K., Goyal, A.K., Mishra, N., Mehta, A., Vyas, S.P.: Effect of lipid core material on characterics of solid lipid nanoparticles designed for oral lymphatic delivery. Nanomed. Nanotechnol. **5**, 184–191 (2009)
6. Noriega-Pelaez, E.K., Mendoza-Munoz, N., Ganem-Quintanar, A., Quintanar-Guerrero, D.: Optimization of the emulsification and solvent displacement method for the preparation of solid lipid nanoparticles. Drug Dev. Ind. Pharm. **37**, 160–166 (2011)
7. Agarwal, S., Pal, D., Mitra, A.K.: Both P-gp and MRP2 mediate transport of Lopinavir, a protease inhibitor. Int. J. Pharm. **339**, 139–147 (2007)
8. Alex, M.R.A., Chacko, A.J., Josea, S., Souto, E.B.: Lopinavir loaded solid lipid nanoparticles (SLN) for intestinal lymphatic targeting. Eur. J. Pharm. Sci. **42**, 11–18 (2011)
9. Negi, J.S., Chattopadhyay, P., Sharma, A.K., Ram, V.: Development of solid lipid nanoparticles (SLNs) of lopinavir using hot self nano-emulsification (SNE) technique. Eur. J. Pharm. Sci. **48**, 231–239 (2013)
10. Miecznik, P., Kaczmarek, M.: Ultrasonic investigations of inclusion complexation of cyclodextrin by iodide ions in pseudobinary aqueous system. J. Mol. Liq. **133**, 120–124 (2007)
11. Chen, W., Yang, L., Ma, S., Yang, X., Fan, B., Lin, J.: Crassicauline A/β-cyclodextrin host-guest system: preparation, characterization, inclusion mode solubilisation and stability. Carbohyd. Polym. **84**, 1321–1328 (2011)

12. Trott, O., Olson, A.J.: AutoDock Vina: improving the speed and accuracy of docking with a new scoring function, efficient optimization and multithreading. J. Comput. Chem. **31**, 455–461 (2010)

13. Srinivasan, K., Stalin, T., Sivakumar, K.: Spectral and electrochemical study of host–guest inclusion complex between 2,4-dinitrophenol and β-cyclodextrin. Spectrochim. Acta A **94**, 89–100 (2012)

14. Varshosaz, J., Ghaffari, S., Khoshayand, M.R., Atyabi, F., Dehkordi, A.J., Kobafard, F.: Optimization of freeze-drying condition of amikacin solid lipid nanoparticles using D-optimal experimental design. Pharm. Dev. Technol. **17**, 187–194 (2012)

15. Kang, J.H., Oh, D.H., Oh, Y., Yong, C.S., Choi, H.: Effects of solid carriers on the crystalline properties, dissolution and bioavailability of flurbiprofen in solid self-nanoemulsifying drug delivery system (solid SNEDDS). Eur. J. Pharm. Biopharm. **80**, 289–297 (2012)

16. Souza, L.G., Silva, E.J., Martins, A.L.L., Mota, M.F., Braga, R.C., Lima, E.M., Valadares, M.C., Taveira, S.F., Marreto, R.N.: Development of topotecan loaded lipid nanoparticles for chemical stabilization and prolonged release. Eur. J. Pharm. Biopharm. **79**, 189–196 (2011)

17. Donato, E.M., Dias, C.L., Rossi, R.C., Valente, R.S., Froehlich, P.E., Bergold, A.M.: LC method for studies on the stability of lopinavir and ritonavir in soft gelatin capsules. Chromatographia **63**, 437–443 (2006)

18. Chen, H., Chang, X., Du, D., Liu, W., Liu, J., Weng, T., Yang, Y., Xu, H., Yang, X.: Podophyllotoxin loaded solid lipid nanoparticles for epidermal targeting. J. Control Release **110**, 296–306 (2006)

19. Shah, M., Chuttani, K., Mishra, A.K., Pathak, K.: Oral solid compritol 888 ATO nanosuspension of simvastatin: optimization and biodistribution studies. Drug Dev. Ind. Pharm. **37**, 526–537 (2011)

20. Wu, H., Liang, H., Yuan, Q., Wang, T., Yan, X.: Preparation and stability investigation of the inclusion complex of sulforaphane with hydroxypropyl-β-cyclodextrin. Carbohyd. Polym. **82**, 613–617 (2010)

21. Yuan, C., Jin, Z., Xu, X.: Inclusion complex of astaxanthin with hydroxypropyl-β-cyclodextrin: UV, FTIR, ^{1}H NMR and molecular modelling studies. Carbohyd. Polym. **89**, 492–496 (2012)

22. Ensikat, H.J., Boese, M., Mader, W., Barthlott, W., Koch, K.: Crystallinity of plant Epicuticular waxes: electron and X-ray diffraction studies. Chem. Phys. Lipids **144**, 45–59 (2006)

23. Hamdi, H., Abderrahim, R., Meganem, F.: Spectroscopic studies of inclusion complex of β-cyclodextrin and benzidine diammonium dipicrate. Spectrochim. Acta A **75**, 32–36 (2010)

24. ^{1}H NMR spectroscopy of fatty acids and their derivatives. http://lipidlibrary.aocs.org/nmr/1NMRsat/index.html/. Accessed 20 Sept 2013

25. Gonil, P., Sajomsang, W., Ruktanonchai, U.R., Pimpha, N., Sramala, I., Nuchuchua, O., Saesoo, S., Chaleawlert-umpon, S., Puttipipatkhachorn, S.: Novel quaternized chitosan containing β-cyclodextrin moiety: synthesis, characterization and antimicrobial activity. Carbohyd. Polym. **83**, 905–913 (2011)

26. Ruz, V., Froeyen, M., Busson, R., Gonzalex, M.M., Baudemprez, L., Mooter, G.V.D.: Characterization and molecular modelling of the inclusion complexes of 2-(2-nitrovinyl) furan (G-0) with cyclodextrines. Int. J. Pharm. **439**, 275–285 (2012)

27. Macedo, O.F.L., Andrade, G.R.S., Conegero, L.S., Barreto, L.S., Costa, N.B., Gimenez, I.F., Almeida, L.E., Kubota, D.: Physicochemical study and characterization of the trimethoprim/2-hydroxypropyl-γ-cyclodextrin inclusion complex. Spectrochim. Acta A **86**, 101–106 (2012)

28. Zhang, Z., Dallek, S., Vogt, R., Li, Y., Topping, T.D., Zhou, Y., Schoenung, J.M., Lavernia, J.: Degassing behavior of nanostructured Al and its composites. Metall. Mater. Trans. A **41**, 532–541 (2010)

29. Li, J., Yan, D., Jiang, X., Chen, Q.: Formation of the crystalline inclusion complex between γ-cyclodextrin and poly (N-acetylethylenimine). Polymer **43**, 2625–2629 (2002)

30. Klang, V., Matsko, N., Raupach, K., El-Hagin, N., Valenta, C.: Development of sucrose stearate-based nanoemulsions and optimisation through γ-cyclodextrin. Eur. J. Pharm. Biopharm. **79**, 58–67 (2011)

31. Das, S., Chaudhury, A.: Recent advances in lipid nanoparticles formulations with solid matrix for oral drug delivery. AAPS PharmSciTech. **12**, 62–76 (2011)

32. Awaad, A., Nakamura, M., Ishimura, K.: Imaging of size-dependent uptake and identification of novel pathways in mouse Peyer's patches using fluorescent organosilica particles. Nanomed. Nanotechnol. **8**, 627–636 (2012)

33. Garg, A., Singh, S.: Enhancement of antifungal activity of eugenol in immunosuppressed rats through lipid nanocarriers. Colloid Surf. B **87**, 280–288 (2011)

34. Vitorino, C., Carvalho, F.A., Almeida, A.J., Sousa, J.J., Pais, A.A.C.C.: The size of solid lipid nanoparticles: an interpretation from experimental design. Colloids Surf. B **84**, 117–130 (2011)